Published in final edited form as:
Neurobiol Aging. 2012 January ; 33(1): 205.e1–205.e18. doi:10.1016/j.neurobiolaging.2010.08.012.

Molecular changes in brain aging and Alzheimer's disease are mirrored in experimentally silenced cortical neuron networks

Marc Gleichmann[a], **Yongqing Zhang**[b], **William H. Wood III**[b], **Kevin G. Becker**[b], **Mohamed R. Mughal**[a], **Michael J. Pazin**[c], **Henriette van Praag**[a], **Tali Kobilo**[a], **Alan B. Zonderman**[d], **Juan C. Troncoso**[e], **William R. Markesbery**[f,1], and **Mark P. Mattson**[a,*]

[a] Laboratory of Neurosciences, National Institute on Aging, Intramural Research Program, Biomedical Research Center, Baltimore, MD, USA

[b] Gene Expression and Genomics Unit, Research Resources Branch, National Institute on Aging, Intramural Research Program, Biomedical Research Center, Baltimore, MD, USA

[c] Laboratory of Cellular and Molecular Biology, National Institute on Aging, Intramural Research Program, Biomedical Research Center, Baltimore, MD, USA

[d] Research Resources Branch, National Institute on Aging, Intramural Research Program, Biomedical Research Center, Baltimore, MD, USA

[e] Department of Pathology, Division of Neuropathology, Johns Hopkins University, School of Medicine, Baltimore, MD, USA

[f] Sanders-Brown Center on Aging, Lexington, KY, USA

Abstract

Activity-dependent modulation of neuronal gene expression promotes neuronal survival and plasticity, and neuronal network activity is perturbed in aging and Alzheimer's disease (AD). Here we show that cerebral cortical neurons respond to chronic suppression of excitability by downregulating the expression of genes and their encoded proteins involved in inhibitory transmission (GABAergic and somatostatin) and Ca^{2+} signaling; alterations in pathways involved in lipid metabolism and energy management are also features of silenced neuronal networks. A molecular fingerprint strikingly similar to that of diminished network activity occurs in the human brain during aging and in AD, and opposite changes occur in response to activation of N-methyl-D-aspartate (NMDA) and brain-derived neurotrophic factor (BDNF) receptors in cultured cortical neurons and in mice in response to an enriched environment or electroconvulsive shock. Our findings suggest that reduced inhibitory neurotransmission during aging and in AD may be the result of compensatory responses that, paradoxically, render the neurons vulnerable to Ca^{2+}-mediated degeneration.

Keywords

Alzheimer's disease; Aging; GABA; Activity; Homeostatic disinhibition; Interneuron; Calcium; Synaptic scaling

[*]Corresponding author at: National Institute on Aging, Intramural Research Program, BRC, 5th Floor, 251 Bayview Blvd, Baltimore, MD 21224, USA. Tel.: +1 410 558 8463; fax: +1 410 558 8465. mattsonm@grc.nia.nih.gov (M. Mattson).
[1]Deceased.

Disclosure statement

The authors have no actual or potential conflict of interest with the work presented in this manuscript.
NIH guidelines were followed for animal usage and for collection of brain tissue.

1. Introduction

Perturbed neuronal network activity occurs early and prior to overt cognitive impairment in Alzheimer's disease (AD) (Sperling et al., 2009). However, the contribution of altered neuronal activity to gene expression changes in the aging brain and in AD is unclear. Evidence exists for both increased and decreased neuronal excitability in AD and in animal models of AD. For example, the frequency of epileptic seizures is increased in AD and mouse models of AD (Larner, 2010; Palop et al., 2007; Scarmeas et al., 2009), and amyloid β-peptide (Aβ) production is increased by neuronal depolarization (Cirrito et al., 2008). Positron emission tomography (PET) and functional magnetic resonance imaging (fMRI) studies indicate that Aβ deposition and memory task-related neuronal activity in the default network area are ranked (greatest to least): AD patients > persons with minimal cognitive impairment > old persons > young persons (Han et al., 2009; Sperling et al., 2009, 2010). Long term potentiation of synaptic transmission, however, is decreased in mouse models of AD (Shankar et al., 2008) and by exposure to Aβ (Hu et al., 2009), and Aβ can reduce seizure-like activity in cultured hippocampal neurons treated with γ-aminobutyric acid (GABA) receptor antagonists (Sepúlveda et al., 2009). However, Aβ has also been shown to increase glutamate-induced cytosolic Ca^{2+} levels (Mattson et al., 1992). No consensus theory has yet emerged to reconcile these seemingly paradoxical features of reduced synaptic transmission and increased excitability in AD.

Microarray studies examining gene expression in AD have been performed by multiple groups over the past decade (Blalock et al., 2004; Colangelo et al., 2002; Emilsson et al., 2006; Ho et al., 2001; Tan et al., 2010; Weeraratna et al., 2007). These studies differed in some details such as using pooled ribonucleic acid (RNA) (Emilsson et al., 2006), using non-AD dementias for the control group (Weeraratna et al., 2007) as well as number of samples, brain regions analyzed, and microarrays used. Consequently, results vary as well, but nevertheless some similarities are present between the studies of Blalock et al. (2004), Emilsson et al. (2006), and Tan et al. (2010).

To test how changes in gene expression that are caused by reduced neuronal activity compare with altered gene expression in AD, we silenced the spontaneous network activity of primary cortical neuron cultures with the Na^{+} channel blocker tetrodotoxin (TTX) and the N-methyl-D-aspartate (NMDA) receptor antagonist MK-801, and compared the results with those from published AD microarray screens. TTX and MK-801 are 2 entirely different chemical entities that are well characterized in their biological actions. Although they act through different molecular targets, their main effect is a severe reduction in neuronal activity. Gene array analysis for both treatments showed a response that is consistent with homeostatic disinhibition, but also showed alterations in Ca^{2+} signaling, and cholesterol and lipid metabolism. The reduction of neuronal activity by TTX and MK-801 in neuron cultures is undoubtedly stronger than occurs in the brains of AD patients. Nevertheless, pathway analysis revealed a significant overlap of gene expression changes in silenced neurons with those seen in AD and the normal aging brain, most obviously for transcripts related to inhibitory neurotransmission. Therefore, disinhibition may be an aspect of altered gene expression in AD and brain aging. Our findings help reconcile the seeming paradox of reduced synaptic transmission and increased excitability, and suggest a potential for therapeutic interventions aimed at improving cognitive performance through direct modulation of neuronal activity.

2. Methods

2.1. Human subjects

Demographics and characteristics of human subjects and brain pathology are summarized in Supplemental Table 1.

2.2. Animals

All animals were housed in compliance with National Institutes of Health (NIH) guidelines. Animal procedures were approved by the National Institute on Aging Animal Care and Use Committee. Environmental enrichment cages (86 × 76 cm) contained rearrangeable toys and tunnels as well as a running wheels for exercise. Control mice were housed in standard cages (30 × 18 cm) devoid of toys and running wheels. Animals were group housed in both conditions (14 mice in environmental enrichment, 6 mice in standard housing). Electroconvulsive shock treatment was performed in 3-month-old C57/B6 mice once a week for 4 weeks with the following settings: 50 mA, 60 Hz, 0.4 ms pulse width and 0.2-second duration. After an isoflurane overdose, animals were decapitated, and brain tissue was quickly removed and frozen on dry ice. Tissue was stored at −80 °C for later protein extraction.

2.3. Neuron culture

Cortical neuron cultures were prepared as described previously (Gleichmann et al., 2009). Neurons were plated at a density of 16,000/cm^2 in Neurobasal medium (Invitrogen, Carlsbad, CA, USA) supplemented with 73.5 M glutamax and B27 (both from Invitrogen). Plating at higher plating densities increased TTX sensitivity (unpublished observation). After the first week 30% medium changes were performed twice weekly. Drugs were substituted only in the freshly added medium. Drugs were used at the following final concentrations: brain derived neurotrophic factor (BDNF) 10 ng/mL (Sigma, St Louis, MO, USA), TTX 1 μM, NMDA 5 μM, MK-801 10 μM, 6-cyano-7-nitroquinoxaline-2,3-dione; FLP 64176, 2,5-Dimethyl-4-[2-(phenylmethyl)benzoyl]-1H-pyrrole-3-carboxylic acid methyl ester (CNQX) 10 μM, Bay K 8644 1 μM, FLP 64176 1 μM (all from Tocris, Ellisville, MO, USA).

2.4. Cell viability test

For viability testing neurons were cultured in 48-well plates. Resazurin (Sigma), the active compound of Alamar blue, was added to a final concentration of 10 μM to the medium from a 500 μM stock solution. After a 30-minute incubation at 37 °C reduction of resazurin was quantified with an HTS 7000 fluorescence plate reader (Perkin Elmer, Waltham, MA, USA) with 560 nm excitation and 590 nm emission. Viability is expressed as % of control.

2.5. RNA isolation and microarray hybridization

RNA isolation and quantification was performed using standard procedures. Quantity and quality control of total RNA samples were performed using the Agilent 2100 bioanalyzer test (Agilent, Santa Clara, CA, USA) for integrity of 18S and 28S RNA bands and by ultraviolet (UV) spectrometry at 260/280 nm. The ratio of 28S to 18S RNA bands was greater or equal to 2.0 for all probes and the 260/280 ratio was greater than 1.8 for all probes. Generation of biotin labeled cloned RNA (cRNA) and microarray hybridization to Illumina's Sentrix RatRef-8 Expression BeadChips (Illumina, San Diego, CA, USA) were performed as described previously (Cheadle et al., 2007). Quantification of the biotin labeled amplified cRNA was done on a Nanodrop 1000 (Nanodrop Products, Wilmington, DE, USA).

2.6. Gene array data analysis

Microarray data were analyzed using DIANE 6.0, a spreadsheet-based microarray analysis program based on SAS JMP 7.0 system (SAS, Cary, NC, USA). Raw microarray data were subjected to filtering and z normalization. Sample quality was analyzed by scatter plot and gene sample *z*-score based hierarchical clustering. Expression changes for individual genes were considered significant if they met 4 criteria: *z*-ratio above 1.5 or below −1.5; false detection rate (FDR) (Tusher et al., 2001) <0.30; *p* value of the pairwise *t* test <0.05; and mean background-corrected signal intensity z score in each comparison group is not negative. These parameters provide a good balance between sensitivity and specificity of the analysis, avoiding excessive representation of false positive and false negative regulation (Cheadle et al., 2003). For pathway analysis the Molecular Signatures database from the BROAD Institute of the Massachusetts Institute of Technology (MIT) was used to calculate z scores (for z-score calculation formula see Supplemental Fig. 1). This procedure has been proven to reliably detect similarities in gene expression signatures across different microarray platforms that may not be apparent by a direct comparison of significantly regulated genes only (Cheadle et al., 2007).

2.7. Immunoblot analysis

Generation of protein lysates and immunoblot analysis were done according to standard procedures. For a list of antibody dilutions and sources see Supplemental Table 2.

2.8. Immunocytochemistry

Immunocytochemistry of paraformaldehyde-fixed (4% in Tris-buffered saline [TBS]) neurons was performed according to standard procedures. Microscopy was performed on a Zeiss (Thornwood, NJ, USA) LSM 510 confocal microscope.

2.9. Calcium imaging

For Ca^{2+} imaging neurons were loaded with 1 μM Fluo8-AM (ABD Bioquest, Sunnyvale, CA, USA) for 15 minutes at 37 °C, and then washed twice in artificial cerebrospinal fluid (ACSF). Time series recordings of Fluo8 fluorescence were performed on a Zeiss LSM 510 confocal microscope with pictures taken in 5-second intervals. During imaging, neurons were maintained in artificial cerebro-spinal fluid (ACSF; in mM: NaCl 120, KCl 3.1, KH_2PO_4 0.4, Tris pH 7.4 20, $NaHCO_3$ 5, $NaSO_4$ 1.2, $CaCl_2$ 1.3, glucose 15).

2.10. Single cell gel electrophoresis (comet assay)

Single cell gel electrophoresis was essentially performed as previously described (Maynard et al., 2008). Assay results (100 cells per sample) were visualized using fluorescence microscopy and analyzed using the Komet 6.0 software (Andor, South Winsor, CT, USA) and mean olive tail moment (OTM) was calculated.

2.11. Chromatin immunoprecipitation

Chromatin immunoprecipitation (ChIP) was performed using methods similar to those described previously (Zhang et al., 2008). Immunoprecipitation was performed with rabbit α-CREB (Santa Cruz Biotechnology, Santa Cruz, CA, USA) or rabbit immunoglobulin G (IgG; Santa Cruz sc-2027). Chromatin was quantified by real-time polymerase chain reaction (PCR) with Sybr green detection (Applied Biosystems, Framingham, MA, USA). Graphs indicate immunoprecipitated chromatin amounts relative to input DNA (percent input). Oligonucleotide sequences are listed in Supplemental Table 3.

3. Results

3.1. Chronic silencing of cortical neuron cultures results in age-dependent delayed cell death

Prolonged treatment with TTX resulted in neuronal cell death that was dependent on both the duration of treatment and the age of the cultures (Fig. 1). If TTX treatment was started at day in vitro (DIV) 7, a 21-day treatment resulted in a ~40% reduction in cell viability (Fig. 1A). If treatment was started at DIV 14 or 21, then 14- or 7-day treatments, respectively, resulted in a similar 40% reduction in viability (Fig. 1A and B). For the remainder of this study TTX treatment was started at DIV 14. Importantly, in this setting no cell death was apparent during the first week of TTX treatment (Fig. 1A). Increased caspase 3 activity after 14 days of TTX treatment is indicative of apoptotic cell death (Fig. 1C), but continuous treatment with caspase or calpain inhibitors did not improve viability (data not shown). Reducing neuronal activity with continuous treatment with 10 μM MK-801, an NMDA receptor channel blocker, for 14 days resulted in an amount of cell death similar to that of TTX-treated cultures. Combined treatment with TTX and MK-801 accelerated cell death after 10 days of treatment, but had little effect on viability after 14 days of treatment (Fig. 1D). Conversely, interventions that facilitate neuronal activity or calcium (Ca^{2+}) influx such as low dose (5 μM) treatment with NMDA and voltage-gated Ca^{2+} channel agonists ameliorated TTX toxicity (Fig. 1E and F). Treatment with BDNF (10 ng/mL) also improved survival, and cotreatment with BDNF and low dose NMDA completely prevented TTX-induced cell death (Fig. 1E). These results indicate that neuronal silencing or activation was the determining factor for cell survival rather than the specific molecular target through which activity was modulated.

3.2. Genes involved in inhibition of excitability are downregulated in chronically silenced neurons

To study the changes in gene expression caused by reduced neuronal activity, messenger RNA (mRNA) isolated from cortical neurons treated with TTX for 3 and 7 days, and from corresponding control cultures (triplicate neuron preparations) was hybridized with Illumina bead rat oligonucleotide microarrays slides. A complete list of significantly regulated genes after 7 days of TTX treatment is shown in Supplemental Table 4; the corresponding Z ratio for the 3-day TTX treatment is also shown in this table. Tables 1 and 2 show the top 30 most down- and up-regulated genes after 7 days of TTX with the corresponding Z ratio for the 3-day treatment included for comparison. From these tables it is apparent that Z ratios for the 3- and 7-day treatment are similar; therefore, for these genes expression at both time points is changing in the same direction.

The top 5 most downregulated mRNAs after 7 days of TTX treatment were (Z ratio in brackets) *somatostatin* (−10.49), *neuropeptide Y* (−8.16), *glutamate decarboxylase 1 (GAD1)* (−7.58), *neurogranin* (−7.54), and *GABA vesicular transporter* (*solute carrier 32a1*) (−6.46). With the exception of neurogranin, all of these mRNAs are exclusively expressed in GABAergic neurons. Other down-regulated transcripts from the top 30 list related to GABAergic neurons or neurotransmission were *Gaba receptor A5*, (−3.84), calbindin 1 (−3.76), and *reelin* (−3.46). *Neurogranin* belongs to the calpacitin family of proteins as does *GAP43* (Z ratio of −3.29) (Table 1). mRNAs encoding enzymes of the cholesterol synthesis pathway formed another group of functionally associated transcripts that were downregulated in silenced neurons. *Farnesyl diphosphate farnesyl transferase* (*Fdft1*, −3.8) and *cytosolic 3-hydroxy-3-methylglutaryl-coenzyme A. synthase* (*HMGCS1*, −3.58) were found in the list of 30 most downregulated genes (Table 1). Additional genes of this pathway with signifi-cant downregulation were *3-hydroxy-3-methylglutaryl-Coenzyme A reductase* (*HMGCR*, −3.58), *farnesyl diphosphate synthase* (*Fdps*, −2.86), *isopentenyl-*

diphosphate delta isomerase (*Idi1*, −2.67), *mevalonate(diphospho) decarboxylase* (*Mvd*, −2.2), and *7-dehydrocholesterol reductase* (*Dhcr7*, −1.96) (Supplemental Table 4). Collectively, these results reveal that chronic neuronal silencing results in prominent reductions in expression of genes involved in GABAergic inhibitory neurotransmission, together with genes involved in calcium signaling and cholesterol metabolism.

The top 30 most upregulated genes in response to neuronal silencing are shown in Table 2. They include genes involved in fatty acid beta oxidation: *carnitine palmitoyltransferase 1* (*Cpt1a*, 3.29) and *acetyl-Coenzyme A dehydrogenase, long-chain* (*Acadl*, 3.27). Other significantly up-regulated transcripts from this pathway included *enoyl coenzyme A. hydratase 1* (*Ech1*, 2.77), *acetyl-Coenzyme A dehydrogenase, medium chain* (*Acadm*, 2.54), *carnitine palmitoyltransferase 2* (*conditions [Cpt2]*, 2.19) and *acyl-Coenzyme A. oxidase 1* (*Acox1*, 1.61) (Supplemental Table 4).

Several functional biological categories of genes affected by TTX-induced neuronal silencing were readily discernible upon examination of the list of most up- and down-regulated cloned DNAs (cDNAs). In order to further interrogate the biological significance of the gene array data, a full pathway analysis of all genes was performed using the molecular signatures database from the BROAD Institute at MIT (Subramanian et al., 2005). For the pathway analysis a Z score was calculated from the Z ratio of all cDNAs in the TTX microarray. A list of all pathways and their Z scores is shown in Supplemental Table 5 and the top 20 most up- and down-regulated pathways are shown in Table 3. Interestingly, the pathway with the highest Z score for downregulated cDNAs was the pathway of cDNAs that are down-regulated in Alzheimer's disease (Z score −10.09), followed by the pathway of cDNAs with downregulated expression in the aging brain (Z score −9.36) and the cholesterol biosynthesis pathway (Z score −8.66). A pathway of downregulated cDNAs in incipient AD also had a high and significant Z score (−5.44). In the pathway analysis of upregulated genes the AD and aging brain pathways again featured prominently with list ranks of 3 and 7, respectively (Z score, 7.06 and 5.68, respectively). The aging brain and AD pathways were described in 2 previous publications that used large samples sizes of brain necropsies to isolate RNA from control and AD patients (Blalock et al., 2004) or from young and old individuals (Lu et al., 2004). The entire list of genes in the "AD down-regulated" pathway with the corresponding Z ratio value from the TTX microarray is shown in Supplemental Table 6. Importantly, the most downregulated mRNAs of the TTX microarray list (somatostatin, neuropeptide Y, GAD1, and neurogranin) were also downregulated in AD. Other mRNAs related to neuropeptide signaling and GABAergic neurons were *vasoactive intestinal peptide*, *GAD2* and *GABA receptor β3*. From the calpacitin family of proteins, *neurogranin*, *GAP43*, and *PCP4* were downregulated in AD and also had a negative Z ratio in the TTX microarray. The entire list of genes in the "aging brain down-regulated" pathway with the corresponding Z ratio value from the TTX microarray is shown in Supplemental Table 7. Of the 122 transcripts downregulated in normal brain aging, 55 had a negative Z ratio and 11 had a positive Z ratio in the TTX microarray. *Somatostatin* and *GAD1* were again included in this list, together with *GABA receptors γ and β 3*. The lists of "AD up-regulated" and "aging brain up-regulated" genes with their corresponding Z ratio from the TTX microarray are shown in Supplemental Tables 8 and 9, respectively.

To confirm the results of the pathway analysis, and to also confirm that the gene expression regulation is dependent on neuronal activity, rather than nonspecific effects of TTX, we isolated RNA from another 3 separate preparations that were either vehicle-treated controls or treated with TTX, MK-801, or TTX plus MK-801 for 7 days. Data analysis showed that the major results from the first microarray analysis were reproduced in that *somatostatin*, neuropeptide Y, *GAD1*, *GAD2*, *GABA vesicular transporter*, *GABA receptors α1*, *α5*, *β2*, *γ2*,

δ, *Thy-1*, *neurogranin*, *pcp4*, *calbindin*, and cholesterol biosynthesis genes were all significantly downregulated by TTX treatment. The corresponding Z ratio values are found in Supplemental Table 10, in which genes are ranked according to their Z ratio comparing TTX treatment to vehicle treatment; Z ratios for the MK-801 and TTX + MK-801 conditions are included for comparison together with *p* values and false detection rate (FDR) values. Comparison of genes downregulated by TTX versus TTX + MK-801 showed that TTX + MK-801 in general resulted in lower Z ratios and *p* values, whereas in the MK-801-treated condition the Z ratios were still negative, but generally higher and not all of them reached significance ($p < 0.05$, indicating a weaker response that was, nonetheless, changed in the same direction; Supplemental Table 8). The pathway analysis of genes downregulated by TTX again showed a strong association with the human aging brain and AD pathways (Z scores −8.32 and −8.24, rank 3 and 5, respectively; Supplemental Table 11). Gene regulation after MK-801 and TTX + MK-801 treatment resulted in very similar Z scores and rankings for the same pathways (Supplemental Table 11). Genes upregulated by TTX treatment also gave high Z score values for AD and the aging brain pathway (Z score 6.90 and 6.40, rank 3 and 8, respectively; Supplemental Table 11). Using a principle component analysis, gene expression profiles were characterized along 3 main axes. This characterization accounted for 73% of the total gene expression variation (Fig. 2). The gene expression profile of control neurons were distinct and separated from all other conditions. Gene expression profiles of neurons treated with TTX or MK-801, however, were located in clusters that extensively overlapped, indicating that their gene expression profiles were highly similar. Combined treatment with TTX and MK-801 resulted in a gene expression profile that was distinct from TTX or MK-801 treatment alone and separated from the expression profile of control neurons by a greater distance than single treatment, likely reflecting a dose-response effect on suppression of neuronal activity.

In conclusion, the results from 2 independent microarray studies, and a total of 6 separate neuron preparations, firmly establish that electrical silencing of cortical neurons results in downregulation of genes involved in GABAergic neurotransmission, inihibitory neuropeptide signaling, genes from the calpacitin family, and genes involved in cholesterol biosynthesis and that this pattern overlaps with a gene expression pattern observed in AD and the human aging brain.

3.3. Electrical silencing decreases levels of inhibition-related proteins in cortical neurons

To confirm that the major changes in gene expression in silenced neurons were associated with corresponding changes at the protein level, we performed immunoblot analysis using antibodies against selected proteins, including GAD1, neurogranin, somatostatin, calbindin and the cholesterol biosynthesis enzymes HMGCR and cHMGCS (also known as HMGCS1). Levels of each of the latter proteins were lower in cortical neurons that had been treated with TTX compared with vehicle-treated control cultures (Fig. 3A and D), consistent with their downregulation in the microarray analysis. Downregulation of HMGCR was weak (79% of control) but reached statistical significance (Fig. 3D). MK-801 treatment for 7 days resulted in reduced expression levels of GAD1, neurogranin, somatostatin, and calbindin. However, in contrast with the microarray results and to TTX treatment, protein levels of HMGCR and HMGCS were not significantly reduced by MK-801. Combined treatment with TTX and MK-801 generally resulted in stronger reductions in the proteins. Cotreatment with TTX and the trophic factor BDNF, despite improved cell viability, caused a decrease in the levels of GAD1, neurogranin, GAP43, calbindin, and cholesterol biosynthesis enzymes to a similar extent as TTX alone. Heme oxygenase 1 (HO-1) mRNA levels were upregulated in response to neuronal silencing (Z ratio 3.09) and, HO-1 protein levels were also increased in response to TTX and decreased by treatment with BDNF and low dose NMDA (Fig. 3A). Importantly, TTX-induced changes in gene and protein expression were not due to an

overall reduction in cell viability or synapse loss, as the expression levels of the synapse marker protein synaptophysin did not decrease after 7 days of TTX treatment (Fig. 3A). However, synaptophysin expression was reduced in neurons treated with TTX plus MK-801, consistent with the accelerated cell death observed in this condition in the viability tests.

Because Ca^{2+} plays major roles as a mediator of activity-dependent changes in neuronal plasticity and survival, we determined the levels of several proteins and protein modifications with an established link to Ca^{2+} signaling. As expected, the levels of the phosphorylated form of the transcription factor cAMP responsive element binding protein (pCREB) were decreased markedly in neurons treated for 7 days with TTX or MK-801, and were partially preserved when brain-derived neurotrophic factor (BNDF) or low dose NMDA were coadministered with TTX (Fig. 3A and D). Interestingly, the expression levels of Ca^{2+}/calmodulin kinase II β (CamKIIβ), classical protein kinase C α-γ (PKC α-γ), and their phosphorylated forms were not reduced by TTX or MK-801 treatment (Fig. 3B and D). Moreover, levels of the stable calpain cleavage product of 150/145 kD of the cytoskeleton protein fodrin (α-II spectrin) was not decreased in electrically silenced neurons; indeed, fodrin proteolysis was increased (Fig. 3B and D). In addition to being cleaved by calpain, fodrin can also be cleaved by caspase 3 to generate a stable breakdown product of 110 kD. TTX treatment for 7 days did not result in generation of the caspase 3-specific cleavage product, again pointing to the absence of apoptotic cell death. Cotreatment with TTX and MK-801 resulted in the appearance of the caspase 3-specific cleavage product of fodrin, consistent with the accelerated cell death observed in this condition (Fig. 3B). Finally, levels of BDNF and the phosphorylated form of its receptor tyrosine kinase B (TrkB) were measured. While BDNF levels increased after BDNF and low dose NMDA treatment, no significant change in BDNF levels was seen after TTX or MK-801 treatment (Fig. 3A). However, levels of the phosphorylated form of TrkB decreased after TTX and MK-801 treatment and increased with BDNF treatment (Fig. 3A and D). Immunocytochemistry confirmed lower expression levels of (nuclear) pCREB, GAD1, and Sst, while pCamKIIβ levels were preserved (Fig. 3C).

3.4. Paradoxical effects of network silencing on neuronal Ca^{2+} homeostasis

Because multiple proteins involved in inhibitory neurotransmission were downregulated in response to electrical silencing, we performed a series of experiments to determine the consequences of electrical silencing on neuronal Ca^{2+} homeostasis. To test whether reduced GABAergic transmission, either through drug application or associated with chronic TTX treatment, resulted in perturbed Ca^{2+} homeostasis in neurons, Ca^{2+} imaging was performed. Cortical neurons in control conditions or treated with TTX for 3–4 days were loaded with the Ca^{2+} sensitive fluorescent indicator fluo-8AM and exposed to increasing concentrations of continuous glutamate in 1 μM steps. Low concentrations of glutamate triggered transient Ca^{2+} spikes in control neurons, and the neurons did not show decompensated Ca^{2+} homeostasis in the presence of 4 μM glutamate (Fig. 4A and B). However, if the GABA (A) receptor antagonist picrotoxin A (50 μM) was added to cells in the presence of 4 μM glutamate, Ca^{2+} homeostasis was lost resulting in a large sustained elevation of the intracellular Ca^{2+} concentration (Fig. 4A and B). In TTX-treated neurons vulnerability to low concentrations of glutamate was significantly increased; concentrations as low as 2 μM frequently caused Ca^{2+} homeostasis to decompensate (Fig. 4C and D). Picrotoxin alone did not cause Ca^{2+} dysregulation but resulted in a slight increase of baseline intracellular Ca^{2+} ($[Ca^{2+}]_i$) (Fig. 4E). Further application of 2 μM glutamate to picrotoxin A-treated neurons resulted in Ca^{2+} dysregulation (Fig. 4E). This demonstrates that in control conditions loss of GABAergic input causes an increase in baseline $[Ca^{2+}]_i$ and increases vulnerability to glutamate-induced Ca^{2+} dysregulation, but does not cause Ca^{2+} dys-regulation by itself. If TTX was washed out from TTX-treated neurons immediately before recording, increased

excitability was observed as indicated by increased spontaneous Ca^{2+} transients (Fig. 4F). In contrast with control conditions, picrotoxin A had no effect and did not increase baseline $[Ca^{2+}]_i$ after TTX washout. The NMDA receptor antagonist MK-801, however, resulted in a loss of spontaneous activity and a decline in baseline $[Ca^{2+}]_i$ (Fig. 4F). These results indicate that after TTX treatment the reduced expression of genes related to GABAergic signaling is associated with a failure to modulate neuronal activity through the GABAergic system, while modulation through the glutamatergic system is comparatively better preserved. Moreover, the increase of baseline $[Ca^{2+}]_i$ and amplitude of $[Ca^{2+}]_i$ transients after TTX washout, and their dependence on glutamatergic activity (Fig. 4F), is indicative of the phenomenon of synaptic scaling, a homeostatic mechanism for synaptic strength (Turrigiano, 2008; Turrigiano et al., 1998). The persistent $[Ca^{2+}]_i$ elevations after glutamate application (Fig. 4A–D), however, is not reversible and therefore represents loss of calcium homeostasis, rather than a controlled increase of calcium transients. In accordance with reduced expression of proteins related to GABAergic transmission, modulation of this system by the GABA (A) receptor agonist muscimol (25 μM) as well as GABA (A) receptor antagonists picrotoxin A (50 μM) and bicuculline (25 μM) had no effect on the viability of TTX-treated neurons (Fig. 4G–I).

3.5. Chronic silencing does not cause oxidative DNA damage in cortical neurons

Oxidative damage to DNA has been implicated in the gene expression changes seen AD and in the aging brain. Specifically, in the aging brain an increase in the 8-oxo-guanine modification in promoter regions was observed, which may result in less efficient transcription (Lu et al., 2004). To test whether neuronal silencing by TTX results in an increase of 8-oxo-guanine residues, single-cell gel electrophoresis (comet assay) was performed in combination with treatment with formamidopyrimidine-DNA glycosylase (fpg), which specifically excises 8-oxo-guanine modifications. Control neurons and neurons treated with TTX for 7 days were used for comet assay. Neurons treated with 10 μM H_2O_2 were used as positive controls. H_2O_2 treatment for 1 hour did not result in cleavage of genomic DNA, as indicated by normal appearance of buffer treated nuclei (Fig. 5A). Incubation with fpg enzyme, however, did produce the typical comet-like shape (Fig. 5A). For quantification the tail moment was determined. While H_2O_2 treatment resulted in a significant increase of the tail moment, TTX did not (Fig. 5B and C). Thus, the changes of mRNA and protein expression caused by electrical silencing of cortical neurons were not associated with increased 8-oxo-guanine formation in genomic DNA.

3.6. Electrical silencing results in reduced binding of CREB to regulatory elements of genes encoding inhibitory proteins

Because CREB is a well-established activity-dependent transcription factor, and because a decrease in levels of its active phosphorylated form was seen in electrically silenced neurons, the functional relevance of reduced pCREB for neuronal gene expression of *GAD1*, *neurogranin*, and *somatostatin* was tested using a chromatin immunoprecipitation assay. TTX treatment for 3 DIV resulted in reduced binding of CREB protein to genomic promoter regions of *GAD1*, *neurogranin*, and *somatostatin*, compared with control neurons (Fig. 5D). Thus, reduced CREB-mediated transcription can in part account for the reduced expression levels of TTX-regulated genes. However, regulation of promoter regions is complex and other factors apart from CREB are likely to contribute to gene expression changes in response to electrical silencing. Notably, the expression patterns of pCREB and TTX-regulated proteins are not completely congruent (Fig. 3A), making it unlikely that CREB is the only relevant transcription factor mediating activity-dependent gene expression.

3.7. Proteins involved in suppression of neuronal excitability are upregulated by increased network activity in vivo

Having established that reduced neuronal activity causes a compensatory reduction in the expression of proteins involved in inhibitory neurotransmission and perturbs Ca^{2+} signaling in cultured cortical neurons, we determined the effects of altered neuronal network activity on protein expression in vivo. Two models were used to increase neuronal activity in vivo, electroconvulsive shock (ECS) and environmental enrichment plus running. GAD1, neurogranin and somatostatin were used as indicators of compensatory responses to increased network activity. ECS (1 treatment per week for 4 weeks) resulted in a marked increase in the levels of GAD1 and neurogranin, and to a lesser extent somatostatin (Fig. 6A and C). Housing in environmental enrichment plus voluntary running caused a clear increase in expression of neurogranin and somatostatin and a less pronounced increase of GAD1 levels (Fig. 6B and D). Thus, the expression of these markers positively correlates with neuronal activity in vitro and in vivo, establishing them as bona fide activity-regulated genes and proteins. Densitometric quantification (Fig. 6C and D) showed significant increases in expression of neurogranin and somatostatin after ECS and environmental enrichment plus running. The increase in GAD1 expression was statistically significant after ECS, whereas the increase after environmental enrichment and running did not reach statistical significance.

3.8. Levels of multiple proteins involved in inhibitory neurotransmission are unchanged in the cerebral cortex and hippocampus in 3xTgAD mice

Our findings above demonstrated that levels of GAD1, neurogranin, and somatostatin are reduced in response to suppression of neuronal activity and are increased in response to neuronal network activation. To elucidate the changes in neuronal network activity in AD we first measured levels of GAD1, neurogranin, and somatostatin in brain tissue samples from the cerebral cortex and hippocampus of 3xTgAD and age-matched nontransgenic mice. 3xTgAD mice express the Swedish mutation of beta-amyloid precursor protein (APP), the presenilin M146V mutation as a knock-in gene, and the tau protein mutation P301L that causes some cases of inherited frontotemporal dementia. These mice exhibit progressive age-dependent Aβ deposits and neurofibrillary tangle-like pathology in their hippocampus and cerebral cortex (Oddo et al., 2003), and associated memory deficits (Halagappa et al., 2007). Hippocampi and cortices were removed from the brains of 23-month-old 3xTgAD mice and wild type congenic control mice and used for immunoblot analysis. There were no apparent differences between 3xTgAD and wild type mice in the levels of GAD1, GAP43 neurogranin, or somatostatin (Fig. 7A, B, D, E). Probing with an antibody against hyperphosphorylated tau protein indicated that the mice were in an advanced stage with prominent accumulation of hyperphosphorylated tau protein (Fig. 7A and B). Protein expression in the hippocampus was also studied in young (6 months) and old (23 months) wild type mice. Again no significant effects of age on the levels GAD1, neurogranin, or somatostatin were observed (Fig. 7C–F).

3.9. Levels of proteins involved in inhibitory neurotransmission are decreased in normal brain aging and AD

Immunoblot analysis was also performed with brain tissue samples from the inferior parietal cortex from Alzheimer's patients and age-matched neurologically normal control subjects. Patient characteristics with postmortem intervals and the method of diagnosis are summarized in Supplemental Table 7. Unlike in the 3xTgAD mice, human AD patients exhibited reductions in GAD1, somatostatin, and neurogranin protein levels (Fig. 8A, B, D). The reduction only partly reflects loss of neurons and synapses in the AD samples, as expression of synaptophysin was not reduced to the same extent (Fig. 8A, B, D). Similar to the observation in TTX-treated cortical neurons, the calpain-specific breakdown product of

fodrin was present in greater amounts in brain tissue samples from AD patients compared with age-matched control subjects (Fig. 8A, B, D).

To determine whether reductions in levels of inhibitory proteins also occurred during normal aging, we measured levels of GAD1, neurogranin and somatostatin in brain tissue samples from neurologically normal control subjects over a wide age range (20–93 years). Demographics of young and old control subjects are summarized in Supplemental Table 7. Levels of GAD1, neurogranin, and somatostatin were lower in brain tissue samples from middle age (35–53 years old) and elderly (68–93 years old) subjects compared with young subjects (≤25 years old) (Fig. 8C and E). Neurogranin was notable in that its levels were much lower in the oldest 3 subjects (71, 80, and 93 years old) compared with all the younger subjects. In 1 elderly (80-year-old) subject the level of GAD1 was elevated, while levels of neurogranin and somatostatin were reduced. When taken together with the results of previous studies (Blalock et al., 2004; Loerch et al., 2008; Lu et al., 2004), our analysis demonstrates that reductions in levels of multiple inhibitory proteins similar to those of AD and normal aging occur in response to experimentally imposed electrical/synaptic silencing in cortical neurons.

4. Discussion

Gene expression profiling of primary cortical neuron cultures revealed a homeostatic disinhibitory response after TTX treatment. Transcripts related to GABAergic interneurons, calpacitins, and cholesterol biosynthesis were significantly downregulated. The activity-dependent nature of this regulation was confirmed in vitro and in vivo and is consistent with findings in the literature (Hendry, 1987; Huang et al., 2006; Lemberger et al., 2008; Rutherford et al., 1997). Importantly, the pathway analysis showed a significant overlap of gene expression changes induced by silencing of cortical neuron cultures with changes observed in AD and the aging brain. Transcripts associated with interneurons and inhibitory neurotransmission were downregulated in both pathways. An apparent implication of these results is that a significant subset of gene expression changes in AD and the aging brain may be caused by impaired excitatory neurotransmission and subsequent homeostatic disinhibition. The exact causes for aging-related impairment of excitatory neurotransmission remain unclear, but increased oxidative damage, reduced metabolic capacity of neurons, and Aβ may be involved. Even though somatostatin has long been recognized as an inhibitory neuropeptide that is downregulated in AD (Beal, 1990; Davies et al., 1980) and activity-dependently expressed (Montminy and Bilezikjian, 1987), a theory of homeostatic disinhibition in the aging brain and in AD has not been formulated. This may be due to the fact that until recently little attention has been focused on interneurons. Also, in AD the focus has often been on direct toxic effects of amyloid plaques, rather than adaptive changes in neuron network activity. However, it has been noted before that direct amyloid toxicity is not a good explanation for reduced expression levels of somatostatin and calbindin in aging and AD as such changes can occur in the absence of amyloid plaques and neuronal death (Geula et al., 2003; Palop et al., 2003; van de Nes et al., 2006). Traditionally interneurons have been regarded as relatively resistant in AD (Young, 1987). Recent evidence from immunohistochemical studies, though, points to clear alterations in interneuron morphology in AD and the aging brain (Knuesel et al., 2009; Koliatsos et al., 2006; Potier et al., 2006; Pugliese et al., 2004; Ramos et al., 2006; Vela et al., 2003) in humans and in rodents. The finding of reduced somatostatin expression in interneurons in subregions of the hippocampus in aged rats and in a mouse model of AD (Potier et al., 2006; Ramos et al., 2006; Vela et al., 2003), contrasts with the results in this study and that of others (Loerch et al., 2008; Savonenko et al., 2005), where no reduction in somatostatin levels was found. This may reflect a lower sensitivity of methods using tissue lysates that were used in the latter studies. The stronger reduction of somatostatin in AD and the aging brain of humans

compared with the corresponding rodent models indicates that overexpression of Aβ in the absence of aging-related changes has a relatively weaker effect on gene expression. Aβ may thus act in a fashion where it will further advance an aging-associated impairment of excitatory neurotransmission.

Recognizing disinhibition of interneurons in AD is important for several reasons. First, disinhibition can explain features of AD and the aging brain, such as increased excitability in the presence of impaired synaptic transmission. Interneurons are the main firewall against epileptic discharges. Thus, a reduction in inhibitory neurotransmission will result in increased vulnerability to seizures and excitotoxicity. Reduced inhibitory neurotransmission also likely will result in a reduced signal-to-noise ratio in information processing and in a reduced ability to generate γ-oscillations, which have been recognized as critical for memory formation and learning (Herrmann and Demiralp, 2005). Thus, disinhibition is likely to contribute to impaired cognitive performance during aging and in AD. On the other hand disinhibition may also be a component of the cognitive reserve, allowing (compensatory) activation of wider brain areas in AD patients and in old persons compared with young persons if the same task is performed. Importantly, the contribution of homeostatic disinhibition of interneurons to cognitive impairment has been recognized in the field of schizophrenia research (Marek et al., 2010). If disinhibition is present in schizophrenia and AD then similar therapeutic strategies aimed at improving cognitive performance can be tested in these conditions, adding a new perspective to AD drug therapy that is independent of Aβ.

One limitation of this study is that similar gene expression regulation does not necessarily have to be mediated through identical mechanisms, i.e., reduced expression of genes related to GABAergic transmission in AD and the aging brain could in principle also be mediated through mechanisms other than homeostatic disinhibition. However, in view of the well characterized inhibitory effects of Aβ on glutamatergic synaptic transmission (Balleza-Tapia et al., 2010; Sepúlveda et al., 2009), we think that homeostatic disinhibition is the most likely mechanism for the down-regulation of genes related to GABAergic transmission in AD. Similarly, in the aging rodent hippocampus a reduction of NMDA receptor-dependent synaptic transmission that correlates with a decline in cognitive function has been reported by different groups (Barnes et al., 2000; Boric et al., 2008; Burke et al., 2008). Also, evidence is emerging that age and Aβ act in concert to impair synaptic transmission (Gengler et al., 2010; Minkeviciene et al., 2008). Such a reduction in NMDA-dependent strength of synaptic transmission would be consistent with subsequent homeostatic disinhibition. In terms of pathogenesis, homeostatic disinhibition is a compensatory mechanism, and as such primarily not pathological in itself, but an indicator of a reduced excitatory drive. Although homeostatic disinhibition is not pathological in itself it most likely comes at the price of increased susceptibility to seizures and glutamate toxicity as well as reduced capacity to generate γ-oscillations. Homeostatic disinhibition can be observed both in the aging (nondemented) brain and in AD, however disinhibition is stronger in AD. This suggests that the aging-associated compensation of reduced excitatory drive is sufficient to retain cognitive function, whereas the additional presence of increased Aβ levels may then exhaust this compensatory mechanism such that cognitive decline accelerates and dementia starts. In this respect it is interesting to speculate on the role that synaptic scaling plays during aging. It might be possible that synaptic scaling is another compensatory mechanism of synaptic plasticity (Turrigiano, 2008) that may then be impaired by Aβ, again resulting in decompensation of cognitive reserve mechanisms.

The AD and aging brain pathways represented in the molecular signatures database of the BROAD institute at MIT are based on the prominently published studies of Blalock et al. (2004; AD pathway) and Lu et al. (2004; aging brain pathway). The significant

downregulation of transcripts related to inhibitory neurotransmission was further corroborated as the most significant change in gene expression of the aging human brain with quantitative reverse transcriptase PCR and immunoblot in a follow-up study to Lu et al. (2004) by Loerch et al. (2008). Also, a recent study by Tan et al. (2010) compared gene expression profiles in the temporal cortex of AD patients and age-matched control persons with separate microarrays for each necropsy. This study found a significant overlap with the gene expression changes reported by Blalock et al. (2004) and Lu et al. (2004) and also found a significant downregulation of GAD1, GAD2, GABA vesicular transporter, somatostatin, 3 GABA A receptor Subunits 1 and 4, as well as calpacitin family members and cholesterol synthesis transcripts. Taken together, our results and the results of the literature indicate that, if conducted carefully, the results of microarray analyses of gene and pathway regulation are reproducible and not coincidence. Moreover, the downregulation of transcripts related to inhibitory neurotransmission is found in multiple areas of human neocortex in AD and the aging brain. On the other hand, this feature is less apparent if microarray analysis is performed in the brain of aging rhesus monkeys and is virtually absent in the aging mouse brain (Loerch et al., 2008), consistent with the findings of this study.

We did not find a significant correlation between levels of protein expression of GAD1, neurogranin and/or (pre-pro)somatostatin (data not shown) and clinical or neuropathological scores. However, the sample size used in the present study is low for correlational studies of this kind and the analysis may not have had sufficient statistical power to reveal such correlations. Notably, the study of Blalock et al. (2004), which used a higher number of samples, did find statistically significant correlations between mRNA expression and Mini Mental Status Examination (MMSE) scores and neurofibrillary tangle score for the following genes: GAD1, GAD2, GAP43, NPY, and SST (negative correlation with neurofibrillary tangle score); GAD1, GAD2, GAP43, NRGN, NPY, PCP4, and SST (positive correlation with MMSE); and PCP4 and SST (positive correlation with MMSE in incipient AD).

Supplementary Material

Refer to Web version on PubMed Central for supplementary material.

Acknowledgments

This work was supported by the Intramural Research Program of the National Institute on Aging. We thank Dr Jenq-Lin Yang for assistance with the comet assay. Brain samples from young control individuals age 20–40 were obtained from the NICHD, Brain and Tissue Bank for Developmental Disorders at the University of Maryland, those from old individuals were provided by the Baltimore Longitudinal Study on Aging. Brain samples from Alzheimer patients and age matched controls were provided from the University of Kentucky Alzheimer's Disease Center Autopsy Program.

The research in this manuscript was funded by the intramural research program of the National Insitute on Aging.

References

Balleza-Tapia H, Huanosta-Gutiérrez A, Márquez-Ramos A, Arias N, Peña F. Amyloid beta oligomers decrease hippocampal spontaneous network activity in an age-dependent manner. Curr Alzheimer Res. 2010; 7:453–462. [PubMed: 20043810]

Barnes CA, Rao G, Houston FP. LTP induction threshold change in old rats at the perforant path – granule cell synapse. Neurobiol Aging. 2000; 21:613–620. [PubMed: 11016529]

Boric K, Muñoz P, Gallagher M, Kirkwood A. Potential adaptive function for altered long-term potentiation mechanisms in aging hippocampus. J Neurosci. 2008; 28:8034–8039. [PubMed: 18685028]

Burke SN, Maurer AP, Yang Z, Navratilova Z, Barnes CA. Glutamate receptor-mediated restoration of experience-dependent place field expansion plasticity in aged rats. Behav Neurosci. 2008; 122:535–548. [PubMed: 18513124]

Beal MF. Somatostatin in neurodegenerative illnesses. Metabolism. 1990; 39:116–119. [PubMed: 1976204]

Blalock EM, Geddes JW, Chen KC, Porter NM, Markesbery WR, Landfield PW. Incipient Alzheimer's disease: microarray correlation analyses reveal major transcriptional and tumor suppressor responses. Proc Natl Acad Sci U S A. 2004; 101:2173–2178. [PubMed: 14769913]

Cheadle C, Vawter MP, Freed WJ, Becker KG. Analysis of microarray data using Z score transformation. J Mol Diagn. 2003; 5:73–81. [PubMed: 12707371]

Cheadle C, Becker KG, Cho-Chung YS, Nesterova M, Watkins T, Wood W 3rd, Prabhu V, Barnes KC. A rapid method for microarray across platform comparisons using gene expression signatures. Mol Cell Probes. 2007; 21:35–46. [PubMed: 16982174]

Cirrito JR, Kang JE, Lee J, Stewart FR, Verges DK, Silverio LM, Bu G, Mennerick S, Holtzman DM. Endocytosis is required for synaptic activity-dependent release of amyloid-beta in vivo. Neuron. 2008; 58:42–51. [PubMed: 18400162]

Colangelo V, Schurr J, Ball MJ, Pelaez RP, Bazan NG, Lukiw WJ. Gene expression profiling of 12633 genes in Alzheimer hippocampal CA1: transcription and neurotrophic factor down-regulation and up-regulation of apoptotic and pro-inflammatory signaling. J Neurosci Res. 2002; 70:462–473. [PubMed: 12391607]

Davies P, Katzman R, Terry RD. Reduced somatostatin-like immunoreactivity in cerebral cortex from cases of Alzheimer disease and Alzheimer senile dementia. Nature. 1980; 288:279–280. [PubMed: 6107862]

Emilsson L, Saetre P, Jazin E. Alzheimer's disease: mRNA expression profiles of multiple patients show alterations of genes involved with calcium signaling. Neurobiol Dis. 2006; 21:618–625. [PubMed: 16257224]

Gengler S, Hamilton A, Hölscher C. Synaptic plasticity in the hippocampus of a APP/PS1 mouse model of Alzheimer's disease is impaired in old but not young mice. PLoS One. 2010; 3:e9764. [PubMed: 20339537]

Geula C, Nagykery N, Wu CK, Bu J. Loss of calbindin-D28K from aging human cholinergic basal forebrain: relation to plaques and tangles. J Neuropathol Exp Neurol. 2003; 62:605–616. [PubMed: 12834105]

Gleichmann M, Collis LP, Smith PJ, Mattson MP. Simultaneous single neuron recording of O2 consumption, $[Ca^{2+}]$i and mitochondrial membrane potential in glutamate toxicity. J Neurochem. 2009; 109:644–655. [PubMed: 19226367]

Halagappa VK, Guo Z, Pearson M, Matsuoka Y, Cutler RG, Laferla FM, Mattson MP. Intermittent fasting and caloric restriction ameliorate age-related behavioral deficits in the triple-transgenic mouse model of Alzheimer's disease. Neurobiol Dis. 2007; 26:212–220. [PubMed: 17306982]

Han SD, Bangen KJ, Bondi MW. Functional magnetic resonance imaging of compensatory neural recruitment in aging and risk for Alzheimer's disease: review and recommendations. Dement Geriatr Cogn Disord. 2009; 27:1–10. [PubMed: 19088472]

Hendry SH, Jones EG. Activity-dependent regulation of GABA expression in the visual cortex of adult monkeys. Neuron. 1987; 1:701–712. [PubMed: 3272185]

Herrmann CS, Demiralp T. Human EEG gamma oscillations in neuropsychiatric disorders. Clin Neurophysiol. 2005; 116:2719–2733. [PubMed: 16253555]

Ho L, Guo Y, Spielman L, Petrescu O, Haroutunian V, Purohit D, Czernik A, Yemul S, Aisen PS, Mohs R, Pasinetti GM. Altered expression of a-type but not b-type synapsin isoform in the brain of patients at high risk for Alzheimer's disease assessed by DNA microarray technique. Neurosci Lett. 2001; 298:191–194. [PubMed: 11165439]

Hu NW, Klyubin I, Anwy R, Rowan MJ. GluN2B subunit-containing NMDA receptor antagonists prevent Abeta-mediated synaptic plasticity disruption in vivo. Proc Natl Acad Sci U S A. 2009; 106:20504–20509. [PubMed: 19918059]

Huang FL, Huang KP, Wu J, Boucheron C. Environmental enrichment enhances neurogranin expression and hippocampal learning and memory but fails to rescue the impairments of neurogranin null mutant mice. J Neurosci. 2006; 26:6230–6237. [PubMed: 16763030]

Knuesel I, Nyffeler M, Mormède C, Muhia M, Meyer U, Pietropaolo S, Yee BK, Pryce CR, LaFerla FM, Marighetto A, Feldon J. Age-related accumulation of Reelin in amyloid-like deposits. Neurobiol Aging. 2009; 30:697–716. [PubMed: 17904250]

Koliatsos VE, Kecojevic A, Troncoso J, Gastard MC, Bennett DA, Schneider JA. Early involvement of small inhibitory cortical interneurons in Alzheimer's disease. Acta Neuropathol. 2006; 112:147–162. [PubMed: 16758165]

Lemberger T, Parkitna JR, Chai M, Schütz G, Engblom D. CREB has a context-dependent role in activity-regulated transcription and maintains cholesterol homeostasis. FASEB J. 2008; 22:2872–2879. [PubMed: 18424767]

Larner AJ. Epileptic seizures in AD patients. Neuromolecular Med. 2010; 12:71–77. [PubMed: 19557550]

Loerch PM, Lu T, Dakin KA, Vann JM, Isaacs A, Geula C, Wang J, Pan Y, Gabuzda DH, Li C, Prolla TA, Yankner BA. Evolution of the aging brain transcriptome and synaptic regulation. PLoS One. 2008; 3:e3329. [PubMed: 18830410]

Lu T, Pan Y, Kao SY, Li C, Kohane I, Chan J, Yankner BA. Gene regulation and DNA damage in the ageing human brain. Nature. 2004; 429:883–891. [PubMed: 15190254]

Marek GJ, Behl B, Bespalov AY, Gross G, Lee Y, Schoemaker H. Glutamatergic (N-methyl-D-aspartate receptor) hypofrontality in schizophrenia: too little juice or a miswired brain? Mol Pharmacol. 2010; 77:317–326. [PubMed: 19933774]

Mattson MP, Cheng B, Davis D, Bryant K, Lieberburg I, Rydel RE. beta-Amyloid peptides destabilize calcium homeostasis and render human cortical neurons vulnerable to excitotoxicity. J Neurosci. 1992; 12:376–389. [PubMed: 1346802]

Maynard S, Swistowska AM, Lee JW, Liu Y, Liu ST, Da Cruz AB, Rao M, de Souza-Pinto NC, Zeng X, Bohr VA. Human embryonic stem cells have enhanced repair of multiple forms of DNA damage. Stem Cells. 2008; 26:2266–2274. [PubMed: 18566332]

Minkeviciene R, Ihalainen J, Malm T, Matilainen O, Keksa-Goldsteine V, Goldsteins G, Iivonen H, Leguit N, Glennon J, Koistinaho J, Banerjee P, Tanila H. Age-related decrease in stimulated glutamate release and vesicular glutamate transporters in APP/PS1 transgenic and wild-type mice. J Neurochem. 2008; 105:584–594. [PubMed: 18042177]

Montminy MR, Bilezikjian LM. Binding of a nuclear protein to the Cyclic AMP response element of the somatostatin gene. Nature. 1987; 328:175–178. [PubMed: 2885756]

van de Nes JA, Konermann S, Nafe R, Swaab DF. Beta-protein/A4 deposits are not associated with hyperphosphorylated tau in somatostatin neurons in the hypothalamus of Alzheimer's disease patients. Acta Neuropathol. 2006; 111:126–138. [PubMed: 16456666]

Oddo S, Caccamo A, Shepherd JD, Murphy MP, Golde TE, Kayed R, Metherate R, Mattson MP, Akbari Y, LaFerla FM. Triple-transgenic model of Alzheimer's disease with plaques and tangles: intra-cellular Abeta and synaptic dysfunction. Neuron. 2003; 39:409–421. [PubMed: 12895417]

Palop JJ, Jones B, Kekonius L, Chin J, Yu GQ, Raber J, Masliah E, Mucke L. Neuronal depletion of calcium-dependent proteins in the dentate gyrus is tightly linked to Alzheimer's disease-related cognitive deficits. Proc Natl Acad Sci U S A. 2003; 100:9572–9577. [PubMed: 12881482]

Palop JJ, Chin J, Roberson ED, Wang J, Thwin MT, Bien-Ly N, Yoo J, Ho KO, Yu GQ, Kreitzer A, Finkbeiner S, Noebels J, Mucke L. Aberrant excitatory neuronal activity and compensatory remodeling of inhibitory hippocampal circuits in mouse models of Alzheimer's disease. Neuron. 2007; 55:697–711. [PubMed: 17785178]

Potier B, Jouvenceau A, Epelbaum J, Dutar P. Age-related alterations of GABAergic input to CA1 pyramidal neurons and its control by nicotinic acetylcholine receptors in rat hippocampus. Neuroscience. 2006; 14:187–201. [PubMed: 16890374]

Pugliese M, Carrasco JL, Geloso MC, Mascort J, Michetti F, Mahy N. Gamma-aminobutyric acidergic interneuron vulnerability to aging in canine prefrontal cortex. J Neurosci Res. 2004; 77:913–920. [PubMed: 15334609]

Ramos B, Baglietto-Vargas D, del Rio JC, Moreno-Gonzalez I, Santa-Maria C, Jimenez S, Caballero C, Lopez-Tellez JF, Khan ZU, Ruano D, Gutierrez A, Vitorica J. Early neuropathology of somatostatin/NPY GABAergic cells in the hippocampus of a PS1xAPP transgenic model of Alzheimer's disease. Neurobiol Aging. 2006; 27:1658–1672. [PubMed: 16271420]

Rutherford LC, DeWan A, Lauer HM, Turrigiano GG. Brain-derived neurotrophic factor mediates the activity-dependent regulation of inhibition in neocortical cultures. J Neurosci. 1997; 17:4527–4535. [PubMed: 9169513]

Savonenko A, Xu GM, Melnikova T, Morton JL, Gonzales V, Wong MP, Price DL, Tang F, Markowska AL, Borchelt DR. Episodic-like memory deficits in the APPswe/PS1dE9 mouse model of Alzheimer's disease: relationships to beta-amyloid deposition and neurotransmitter abnormalities. Neurobiol Dis. 2005; 18:602–617. [PubMed: 15755686]

Scarmeas N, Honig LS, Choi H, Cantero J, Brandt J, Blacker D, Albert M, Amatniek JC, Marder K, Bell K, Hauser WA, Stern Y. Seizures in Alzheimer disease: who, when, and how common? Arch Neurol. 2009; 66:992–997. [PubMed: 19667221]

Sepúlveda FJ, Opazo C, Aguayo LG. Alzheimer beta-amyloid blocks epileptiform activity in hippocampal neurons. Mol Cell Neurosci. 2009; 41:420–428. [PubMed: 19427381]

Shankar GM, Li S, Mehta TH, Garcia-Munoz A, Shepardson NE, Smith I, Brett FM, Farrell MA, Rowan MJ, Lemere CA, Regan CM, Walsh DM, Sabatini BL, Selkoe DJ. Amyloid-beta protein dimers isolated directly from Alzheimer's brains impair synaptic plasticity and memory. Nat Med. 2008; 14:837–842. [PubMed: 18568035]

Sperling RA, Laviolette PS, O'Keefe K, O'Brien J, Rentz DM, Pihlajamaki M, Marshall G, Hyman BT, Selkoe DJ, Hedden T, Buckner RL, Becker JA, Johnson KA. Amyloid deposition is associated with impaired default network function in older persons without dementia. Neuron. 2009; 63:178–188. [PubMed: 19640477]

Sperling RA, Dickerson BC, Pihlajamaki M, Vannini P, LaViolette PS, Vitolo OV, Hedden T, Becker JA, Rentz DM, Selkoe DJ, Johnson KA. Functional alterations in memory networks in early Alzheimer's disease. Neuromol Med. 2010; 12:27–43.

Subramanian A, Tamayo P, Mootha VK, Mukherjee S, Ebert BL, Gillette MA, Paulovich A, Pomeroy SL, Golub TR, Lander ES, Mesirov JP. Gene set enrichment analysis: a knowledge-based approach for interpreting genome-wide expression profiles. Proc Natl Acad Sci U S A. 2005; 102:15545–15550. [PubMed: 16199517]

Tan MK, Chua WT, Esiri MM, Smith AD, Vinter HV, Lai MK. Genome wide profiling of altered gene expression in the neocortex of Alzheimer's Disease. J Neurosci Res. 2010; 88:1157–1169. [PubMed: 19937809]

Turrigiano GG, Leslie KR, Desai NS, Rutherford LC, Nelson SB. Activity-dependent scaling of quantal amplitude in neocortical neurons. Nature. 1998; 391:892–896. [PubMed: 9495341]

Turrigiano GG. The self-tuning neuron: synaptic scaling of excitatory synapses. Cell. 2008; 135:422–435. [PubMed: 18984155]

Tusher VG, Tibshirani R, Chu G. Significance analysis of microarrays applied to the ionizing radiation response. Proc Natl Acad Sci U S A. 2001; 98:5116–5121. [PubMed: 11309499]

Vela J, Gutierrez A, Vitorica J, Ruano D. Rat hippocampal GABAergic molecular markers are differentially affected by ageing. J Neurochem. 2003; 85:368–377. [PubMed: 12675913]

Weeraratna AT, Kalehua A, Deleon I, Bertak D, Maher G, Wade MS, Lustig A, Becker KG, Wood W 3rd, Walker DG, Beach TG, Taub DD. Alterations in immunological and neurological gene expression patterns in Alzheimer's disease tissues. Exp Cell Res. 2007; 313:450–461. [PubMed: 17188679]

Young AB. Cortical amino acidergic pathways in Alzheimer's disease. J Neural Transm Suppl. 1987; 24:147–152. [PubMed: 2824688]

Zhang P, Pazin MJ, Schwartz CM, Becker KG, Wersto RP, Dilley CM, Mattson MP. Nontelomeric TRF2-REST interaction modulates neuronal gene silencing and fate of tumor and stem cells. Curr Biol. 2008; 18:1489–1494. [PubMed: 18818083]

Appendix. Supplementary data

Supplementary data associated with this article can be found, in the online version, at doi: 10.1016/j.neurobiolaging.2010.08.012.

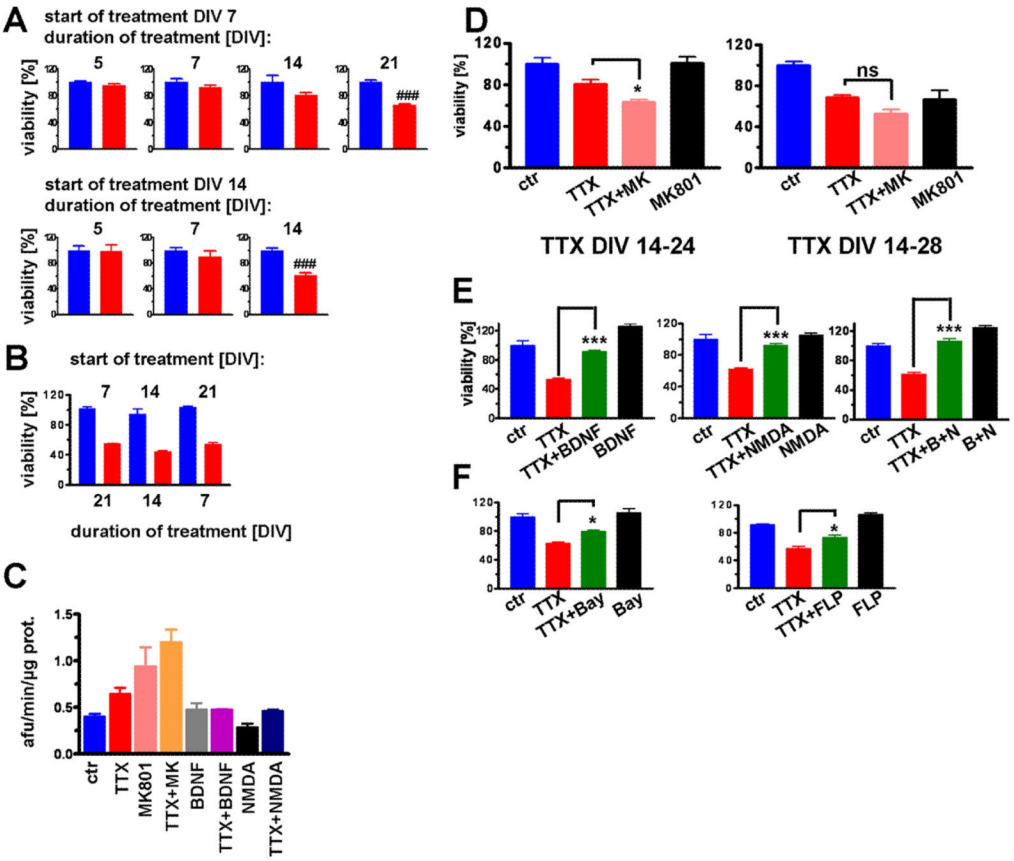

Fig. 1.

Impact of chronic silencing of network activity on the viability of cerebral cortical neurons is time- and cell state-dependent. (A) Vulnerability to tetrodotoxin (TTX) increased with age in culture. When TTX was started on day in vitro (DIV) 7 (upper panel), viability was reduced by 40% after 21 days of treatment. When TTX was started on DIV 14 (lower panel), viability was reduced by 40% after 14 days of treatment. (B) When TTX was started at 21 DIV, viability was reduced by 40% after 7 days of treatment. (C) Caspase 3 activity increased after 14 days of treatment with TTX and or MK-801, but not if brain-derived neurotrophic factor (BDNF) or 5 μM N-methyl-D-aspartate (NMDA) were coadministered. (D) TTX treatment in combination with MK-801 accelerated cell death compared with either treatment alone (left chart, 10 days of treatment), but had little effect after 14 days of treatment (right chart). (E) Treatment with BDNF (left graph) as well as 5 μM NMDA (middle graph) resulted in increased viability when compared with control. Cotreatment with TTX and NMDA completely prevented TTX-induced toxicity (right graph). (F) Similarly, cotreatment of TTX with Ca^{2+} agonists Bay K 8644 or FLP 64176 (1 μM) or TTX resulted in ameliorated conditions ($^{###}p < 0.001$ *t*-test; $^{*}p < 0.05$ and $^{***}p < 0.001$ analysis of variance [ANOVA] with Tukey posthoc test).

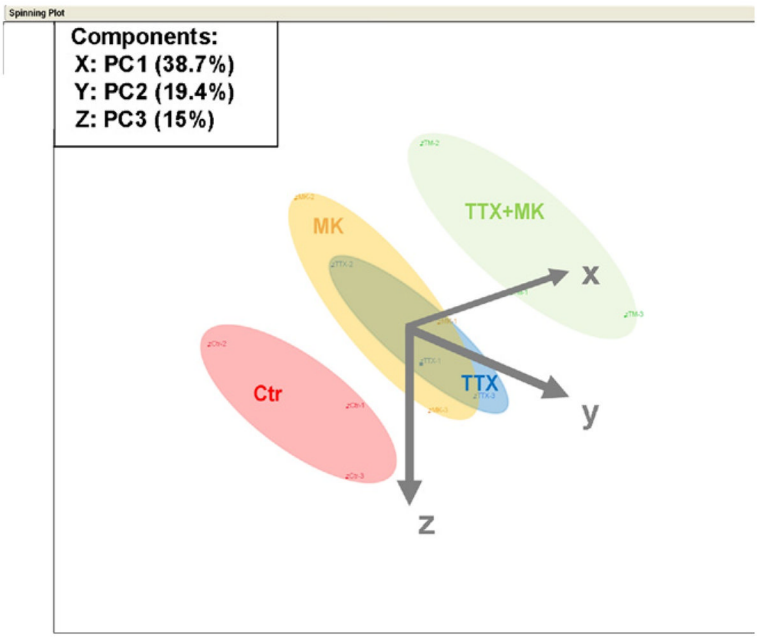

Fig. 2.

Silencing of intrinsic neuronal activity and glutamatergic synaptic transmission results in similar changes in gene expression compared with electrically active control neurons. Results of a principle component analysis displayed as 3-dimensional diagram along 3 axes. Each point represents the specific gene expression profile in this space for 3 replicates of neurons in control conditions (Ctr), tetrodotoxin treatment (TTX), MK-801 treatment (MK), or combined TTX and MK-801 treatment (TTX+MK). The expression profile of control neurons locates in a cluster that is distinct from all other conditions. TTX and MK-801 treatment cause gene expression profiles that are highly similar and locate in overlapping clusters. Combined treatment with TTX and MK-801 results in a distinct gene expression profile cluster that is more distant from control neurons than TTX or MK-801 treatment alone.

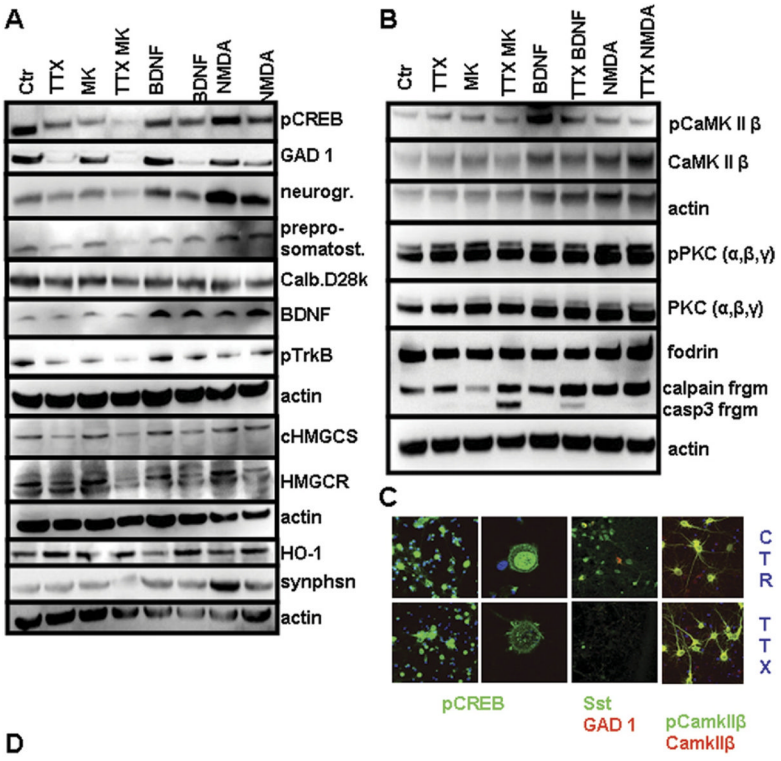

D

	pCreb	GAD 1	Nrgn	ppSst	Calb.	pTrk B	cHMG CS	HMGC R	HO-1	pCaMKII to CamKII ratio	pPKC to PKC ratio	calpain frgm ratio
TTX	47 (17)	20 (5)	67 (27)	62 (16)	71 (2)	48 (2)	32 (18)	79 (6)	180 (38)	103 (139)	99 (21)	19 (3)
MK801	29 (14)	47 (9)	54 (22)	50 (19)	76 (13)	35 (7)	90 (37)	99 (3)	190 (90)	109 (21)	89(9)	17 (6)
n number	3	3	4	5	3	3	3	3	3	3	3	3
p value TTX	0.006	1E-04	0.0502	7E-04	1E-04	1E-04	0.0028	0.0037	0.0218	0.972	0.9382	0.0309
p value MK	9E-04	5E-04	0.0058	4E-04	0.033	1E-04	0.6641	0.5946	0.1583	0.7423	0.1017	0.1963

Fig. 3.

Chronic silencing of cortical neurons results in decreased levels of multiple proteins involved in inhibitory neurotransmission, as well as reduced levels of activated CREB. (A) pCREB, GAD1, neurogranin, preprosomatostatin, GAP43, calbindin D28k, BDNF, pTrkB, cHMGCS, HMGCR, heme oxygenase 1 and synaptophysin protein levels in cultured cortical neurons that had been exposed to the indicated treatments for 7 days. (B) Protein levels and phosphorylation levels of CamKII and PKC as well as fodrin cleavage pattern after tetrodotoxin (TTX) treatment. (C) Immunocytochemical analysis of pCREB, GAD1, total PKC and pPKC immunoreactivities confirms the immunoblot data (panels A and B). (D) Densitometric quantification of immunoblots after TTX and MK-801 treatment are presented as % of control (SD) with corresponding *p* values for *t*-test. Values for brain-derived neurotrophic factor (BNDF) and synaptophysin did not show a significant reduction and are left out because of space limitation. Calpain fragment densitometry is expressed as % of total calpain (full-length + calpain + caspase fragment). Complete densitometric quantification of immunoblots can be found in Supplemental Table 12.

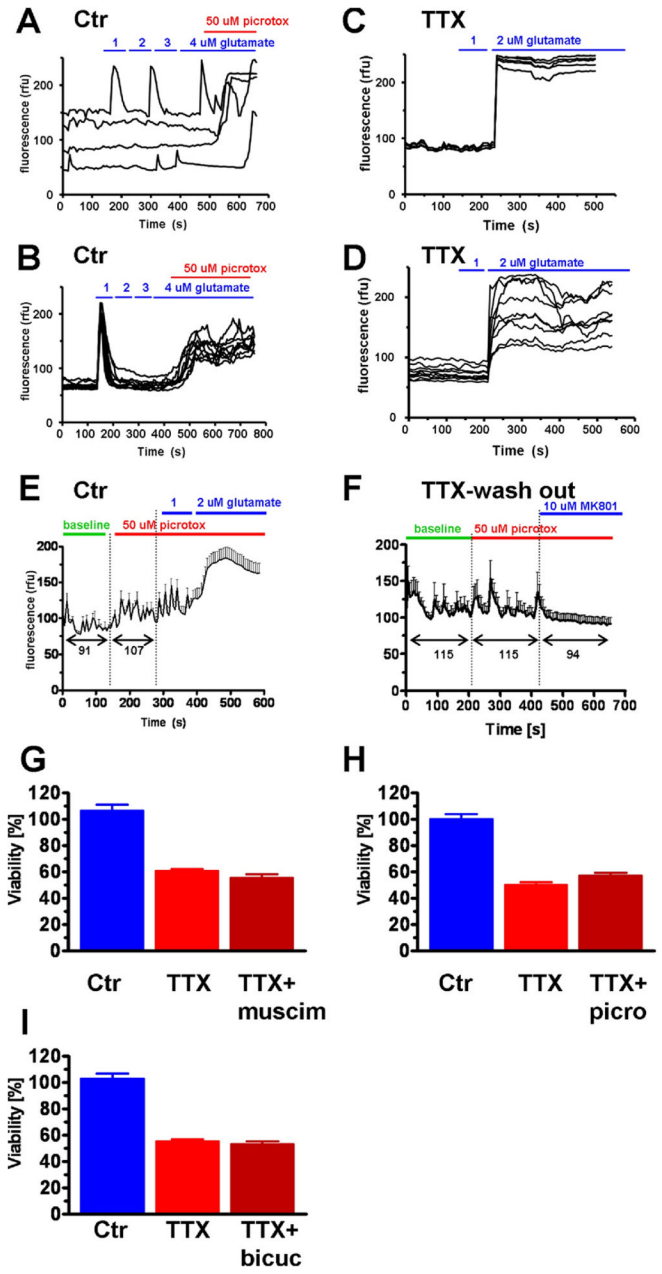

Fig. 4.

Ca^{2+} imaging studies reveal that chronic silencing of neurons increases their excitability. (A and C) Control neurons showed either no response or short Ca^{2+} transients with return to baseline intracellular Ca^{2+} ($[Ca^{2+}]_i$) after incremental additions of 1 μM glutamate up to a total concentration of 4 μM. Further addition of γ-aminobutyric acid (GABA) receptor antagonist picrotoxin A (50 μM), however, resulted in Ca^{2+} dysregulation. (B and D). After 3 days of TTX treatment, glutamate doses of 2 μM resulted in a loss of Ca^{2+} homeostasis indicated by a sustained elevation of $[Ca^{2+}]_i$. (E) In control neurons GABA receptor antagonist picrotoxin A (50 μM) alone caused a small increase in $[Ca^{2+}]_i$ but no Ca^{2+} dysregulation. Additional application of 2 μM glutamate resulted in Ca^{2+} dysregulation. Black numbers below arrow bars indicate mean fluorescent intensity during baseline and after 50 μM picrotoxin A. (F) In TTX neurons where TTX was washed out before the

recording spontaneous activity was increased under baseline conditions but picrotoxin A had no effect on this activity or on $[Ca^{2+}]_i$. MK-801, however, silenced neuronal activity and caused a reduction in $[Ca^{2+}]_i$. Black numbers below arrow bars indicate mean fluorescent intensity during baseline, after addition of 50 μM picrotoxin A and after addition of MK-801. (G–I) Neither GABA receptor agonist muscimol (25 μM) (G), nor the GABA receptor antagonists picrotoxin A (50 μM) (H), or bicuculline (25 μM) (I) changed TTX-induced loss of neuronal viability after 14 days of treatment.

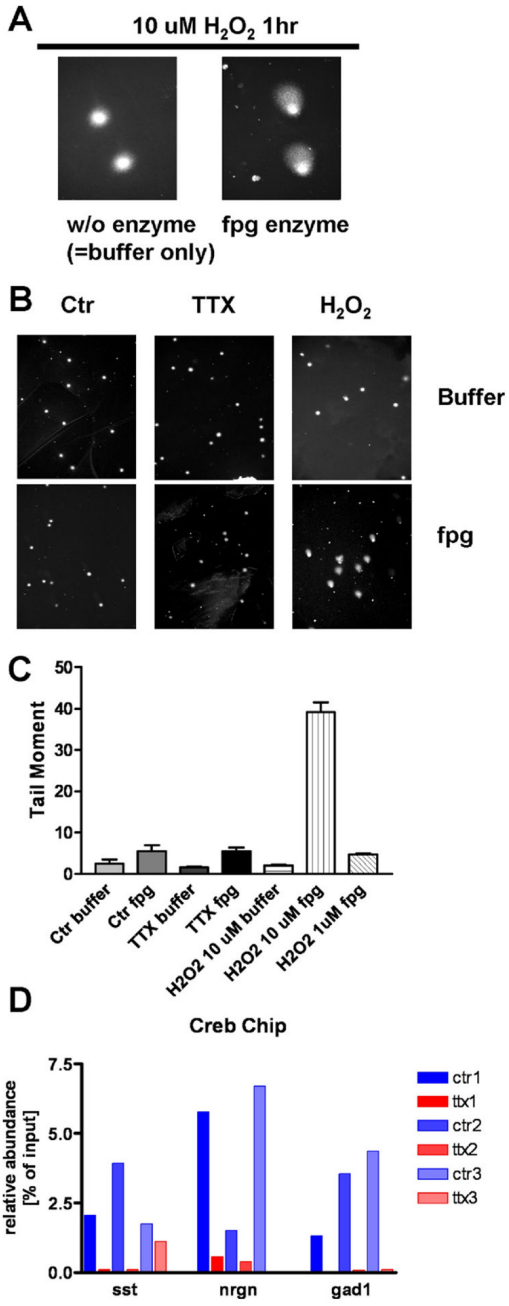

Fig. 5.

Absence of increased oxidative (8-oxo guanine) DNA modifications in electrically silenced cortical neurons and activity-dependent binding of CREB to genomic promoter regions of *GAD1*, Sst and *nrgn*. (A) Positive control experiment demonstrates that genomic 8-oxo guanine modifications were induced by a 1-hour treatment with 10 μM H_2O_2. No comet-like structures were seen in the absence of formamidopyrimidine-DNA glycosylase (fpg) digestion, indicating the absence of DNA fragmentation. After digestion with fpg comet-like structures appeared, revealing 8-oxo guanine genomic modifications. (B) Representative pictures showing that H_2O_2 for 1 hour, but not tetrodotoxin (TTX) treatment for 7 days, resulted in the appearance of comet-like structures. (C) Quantification of the tail moment of 100 neurons per condition showed no increase in tail moment after TTX for 7 days. (D)

Chromatin immunoprecipitation (ChIP) of genomic DNA from TTX-treated and control neurons was performed with a CREB antibody. qPCR of promoter regions of *somatostatin* (A), *neurogranin* (B) and *GAD1* (C) genes in 3 separate neuron preparations show consistently lower CREB binding to promoter sites after TTX treatment.

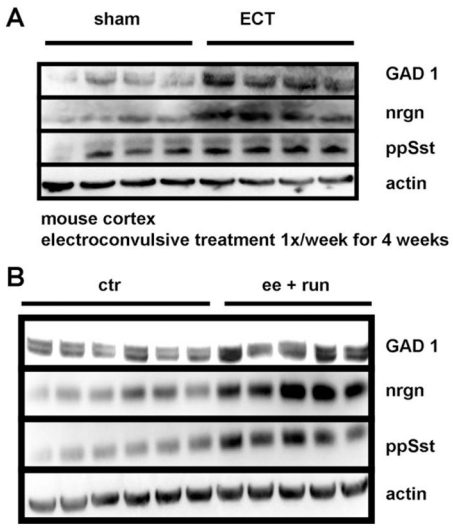

C

	sham	ECT	t-test
GAD1	100 (24)	311 (34)	**p=0.0011**
Nrgn	100 (21)	241 (20)	**p=0.0014**
ppSst	100 (38)	223 (26)	**p=0.0207**

D

	Ctr	Env. Enr.+ Run	t-test
GAD1	100 (7)	148 (33)	p=0.111
Nrgn	100 (22)	208 (37)	**p=0.016**
ppSst	100 (24)	241 (27)	**p=0.019**

Fig. 6.

Neuronal activity increases the expression of GAD1, somatostatin, and neurogranin in vivo. (A) Neuronal activity in vivo was increased by electroconvulsive shock (ECS) once per week for 4 weeks, resulting in increased protein expression of GAD1, preprosomatostatin (pp Sst) and neurogranin (nrgn) compared with sham treated animals. (B) Neuronal activity in vivo was increased by housing in environmentally enriched cages with running wheels (ee + run) or conventionally housed animals resulted in increased protein expression of GAD1, preprosomatostatin (pp Sst) and neurogranin (nrgn). (C and D) Densitometric quantification of immunoblots. Average densitometric intensity (+ SEM) displayed as percent of sham treated animals (C) or control housed animals (D) with corresponding *p* values for *t*-test. Bold *p* values indicate statistical significant differences.

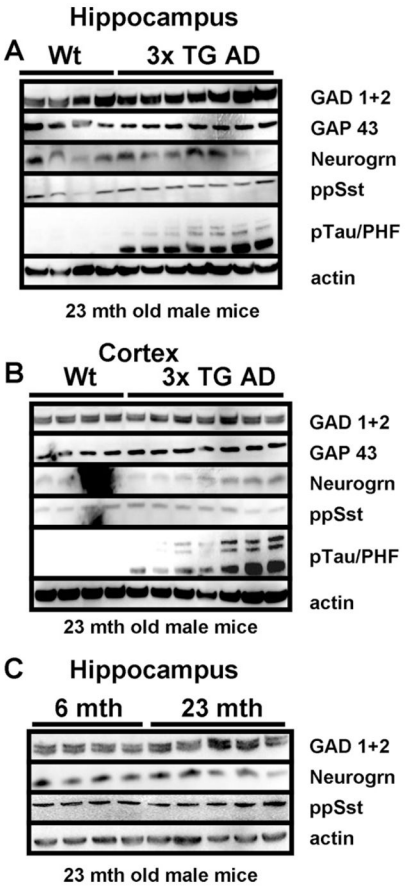

D

	Wt	3 x TG AD	t-test
GAD1	100 (0)	105 (4)	p=0.3588
GAP43	100 (64)	132 (35)	p=0.5992
Nrgn	100 (24)	108 (19)	p=0.7724
ppSst	100 (35)	81 (13)	p=0.5083

E

	Wt	3 x TG AD	t-test
GAD1	100 (12)	123 (16)	p=0.3064
GAP43	100 (19)	132 (8)	p=0.0675
Nrgn	100 (20)	84 (10)	p=0.4545
ppSst	100 (46)	130 (35)	p=0.5823

F

	6mth	23 mth	t-test
GAD1	100 (7)	109 (19)	p=0.6063
Nrgn	100 (1)	94 (6)	p=0.3263
ppSst	100 (5)	92 (22)	p=0.6899

Fig. 7.

Levels of proteins involved in inhibitory neurotransmission are unchanged in the cortex and hippocampus of a mouse model of Alzheimer's disease. (A and B) Levels of GAD1, GAP43, neurogranin (nrgn), and preprosomatostatin (pp Sst) did not differ in the hippocampus (A) or cortex (B) between 23-month-old male wild type and 3xTgAD mice. Levels of phosphorylated tau protein were elevated in the 3xTgAD mice, indicating their advanced stage of disease. (C) Levels of GAD1, GAP43, neurogranin, and preprosomatostatin in the hippocampus did not differ between 6-month-old and 23-month-old wild type mice. (D, E, and F) Densitometric quantification of immunoblots. Average densitometric intensity (+ SEM) displayed as percent of wild type animals (D and E) or 6-month-old animals (D) with corresponding *p* values for *t*-test. Bold *p* values indicate statistical significant differences.

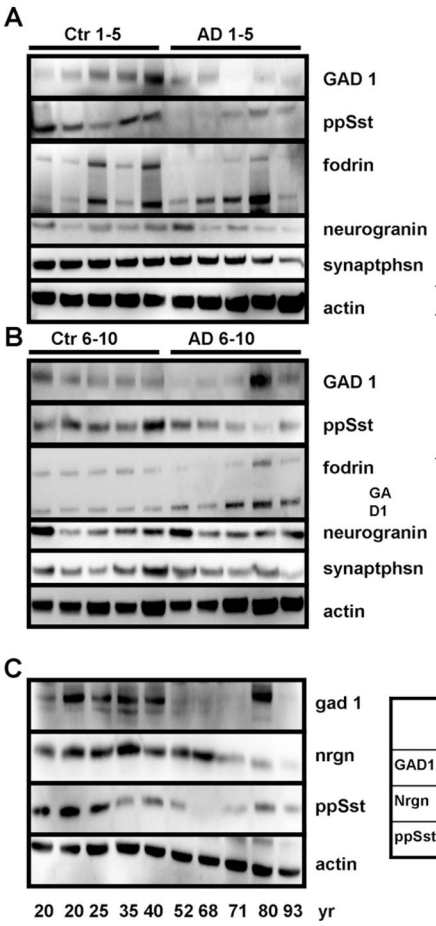

D

	Ctr	AD	t-test
GAD1	100 (7)	73 (14)	p=0.0911
ppSst	100 (12)	21 (4)	**p<0.0001**
fodrin	58 (3)	71 (4)	**p=0.0214**
Nrgn	100 (22)	52 (8)	**p=0.0473**
synphsn	100 (12)	68 (11)	**p=0.0488**

E

	20 yr	20 yr	25 yr	35 yr	40 yr	52 yr	68 yr	71 yr	80 yr	93 yr
GAD1	125	161	134	224	113	25	26	31	123	37
Nrgn	110	203	185	161	90	72	87	30	49	13
ppSst	193	202	176	73	96	54	7	12	74	13

Fig. 8.

Levels of activity-dependent proteins are reduced in Alzheimer's disease (AD) and in the neurologically normal human brain during aging. (A and B) Levels of GAD1, neurogranin (nrgn), and preprosomatostatin (pp Sst) were reduced in the inferior parietal cortex of AD patients compared with age-matched controls. (C) Levels of GAD1, neurogranin and preprosomatostatin in the cerebral cortex of neurologically normal individuals of the indicated ages (20–93 years). (D and E) Densitometric quantification of immunoblots. Average densitometric intensity (± SEM) displayed as percent of nondemented subjects with corresponding *p* values for *t*-test (D) or as percent of the average intensity across all ages (E). Bold *p* values indicate statistical significant differences.

Table 1

TTX downregulated genes

Definition	Z ratio	
	7 DIV vs. control	3 DIV vs. control
Somatostatin (Sst)	−10.49	−9.09
Neuropeptide Y (npy)	−8.16	−7.09
Glutamate decarboxylase 1 (Gad1)	−7.58	−6.68
Neurogranin (Nrgn)	−7.54	−3.78
Solute carrier family 32 (GABA vesicular transporter), member 1 (Slc32a1)	−6.46	−4.48
Thymus cell antigen 1, theta (Thy1)	−5.65	−3.79
Similar to cyclin-dependent kinase 5 activator isoform p39 precursor (LOC5011)	−5.18	−3.91
Brain-enriched SH3-domain protein Besh3 (Besh3)	−4.42	−3.77
NEL-like 1 (chicken) (Nell1)	−4.06	−2.84
Similar to contains transmembrane (TM) region (predicted) (LOC361560)	−3.99	−3.25
Eukaryotic translation elongation factor 1 alpha 2 (Eef1a2)	−3.91	−1.13
Gamma-aminobutyric acid A receptor, alpha 5 (Gabra5)	−3.84	−3.48
Famesyl diphosphate famesyl transferase 1 (Fdft1)	−3.8	−3.58
Neuropilin (NRP) and tolloid (TLL)-like 2 (predicted) (Neto2_predicted)	−3.78	−3.22
Calbindin 1 (Calb1)	−3.76	−4.51
Similar to Ca^{2+}-dependent activator for secretin protein 2 (LOC312166)	−3.62	−4.55
IQ motif and Sec7 domain 3 (lqsec3)	−3.61	−4.08
Rho GDP dissociation inhibitor (GDI) gamma (predicted) (Arhgdig_predicted)	−3.6	−2.89
3-hydroxy-3methylglutaryl-Coenzyme A synthase 1 (Hmgcs1)	−3.58	−3.4
Reelin (Reln)	−3.48	−4.55
Visinin-like 1 (Vsnl1)	−3.46	−4.92
Chimerin (chimaerin) 1 (Chn1)	−3.46	−3.3
Calcium/calmodulin-dependent protein kinase II inhibitor 1 (Camk2n1)	−3.44	−0.71
Stathmin-like 3 (Stmn3)	−3.37	−0.86
Calcium/calmodulin-dependent protein kinase II beta subunit (Camk2b)	−3.35	−2.38
Growth associated protein 43 (Gap43)	−3.29	−0.52
N-myc downstream regulated 4 (Ndr4)	−3.27	−2.25
Similar to TAFA1 protein (LOC500266)	−3.26	−2.94
ATPase, H^+ transporting, V1 subunit G isoform 2 (Atp6v1g2)	−3.24	−2.66
Ubiquitin carboxy-terminal hydrolase L1 (Uchl1)	−3.23	−1.92

The most strongly downregulated genes after 7 days of TTX treatment ranked according to their Z ratio. Z ratios after 3 days of TTX treatment are listed for comparison.

Key: DIV, days in vitro; TTX, tetrodotoxin.

Table 2

TTX upregulated genes

Definition	Z ratio	
	7 DIV vs. control	3 DIV vs. control
Similar to LRRG00135 (LOC501637)	5.55	4.8
Similar to LRRG00135 (LOC501548)	5.49	5.16
Ectonucleoside triphosphate diphosphohydrolase 2 (Entpd2)	4.09	0.99
2,4-dienoyl CoA reductase 1, mitochondrial (Decr1)	3.91	3.03
Heat-responsive protein 12 (Hrsp12)	3.8	1.52
Phospholipase A2, group VII (platelet-activating factor acetylhydrolase, plasma) (Pla2)	3.76	3.93
Cytochrome P450, family 7, subfamily b, polypeptide 1 (Cyp7b1)	3.74	‘2.87
Steroid sensitive gene 1 (Ssg1)	3.7	1.09
Monoamine oxidase B (Maob)	3.7	3.43
HRAS-like suppressor (Hrasls3)	3.68	2.89
S100 calcium binding protein A1 (S100a1)	3.55	4.74
Pirin (Pir)	3.52	2.4
Plasminogen activator, tissue (Plat)	3.49	0.81
Hypothetical gene supported by NM_178095 (LOC497803)	3.48	2.4
Similar to NDP (LOC363443)	3.44	3.07
F-box only protein 2 (Fbxo2)	3.44	3.19
Insulin-like growth factor binding protein 7 (predicted) (lgfbp7_predicted)	3.41	2.49
Solute carrier family 4, member 2 (Slc4a2)	3.34	2.97
Carnitine palmitoyltransferase 1, liver (Cpt1a)	3.29	2.54
Similar to transmembrane 4 superfamily member 6 (LOC302313)	3.27	0.25
Acetyl-Coenzyme A dehydrogenase, long-chain (Adadl)	3.27	2.71
Sterol carrier protein 2 (Scp2)	3.23	0.7
Complement component 1, q subcomponent-like 1 (predicted) (C1ql1_predicted)	3.23	2.11
Aldehyde oxidase 1 (Aox1)	3.23	2.62
Matrix metalloproteinase 14 (membrane-inserted) (Mmp14)	3.23	3.01
Hypothetical LOC362870 (LOC362870)	3.22	3.08
Carbonic anhydrase 2 (Ca2)	3.17	1.51
Paraoxonase 2 (predicted), mRNA (cDNA clone MGC:95017 IMAGE:7122087)	3.17	1.68
Similar to Glutathione S-transferase 8 (GST 8-8) (Chain 8) (GST class-alpha) (LOC 50)	3.17	3.45
Gamma-aminobutyric acid A receptor, gamma 1 (Gabrg1)	3.15	1.02

The most strongly upregulated genes after 7 days of TTX treatment ranked according to their Z ratio. Z ratios after 3 days of TTX treatment are listed for comparison.

Key: DIV, days in vitro; TTX, tetrodotoxin.

Table 3

TTX regulated pathways

Pathway name	Z score	
	7 DIV vs. control	3 DIV vs. control
Twenty most strongly downregulated		
AGEING_BRAIN_DOWN	−10.09	−9.84
ALZHEIMERS_DISEASE_DOWN	−9.36	−11.15
CHOLESTEROL_BIOSYNTHESIS	−8.66	−8.73
CALCIUM_REGULATION_IN_CARDIAC_CELLS	−7.40	−7.47
PGC1APATHWAY	−6.63	−4.47
SMOOTH_MUSCLE_CONTRACTION	−6.38	−6.85
CACAMPATHWAY	−5.98	−4.41
CPR_LOW_LIVER_UP	−5.97	−5.40
DFOSB_BRAIN_2WKS_UP	−5.85	−6.62
TERPENOID_BIOSYNTHESIS	−5.75	−5.77
CREB_BRAIN_2WKS_UP	−5.71	−5.00
TPA_RESIST_LATE_UP	−5.65	−2.82
COCAINE_BRAIN_5D_UP	−5.50	−4.44
NOS1PATHWAY	−5.46	−4.06
CREB_BRAIN_8WKS_UP	−5.45	−4.96
ALZHEIMERS_INCIPIENT_DOWN	−5.44	−5.29
HIPPOCAMPUS_DEVELOPMENT_POSTNATAL	−5.32	−3.10
BIOSYNTHESIS_OF_STEROIDS	−5.19	−5.19
HDACPATHWAY	−4.79	−3.93
GPCRPATHWAY	−4.75	−4.22
Twenty most strongly upregulated		
STEMCELL_NEURAL_UP	8.40	3.69
RUTELLA_HEMATOGFSNDCS_DIFF	7.58	2.51
ALZHEIMERS_DISEASE_UP	7.06	4.79
BRCA_ER_NEG	6.28	3.53
RUTELLA_HEPATGFSNDCS_UP	7.06	4.79
MITOCHONDRIAL_FATTY_ACID_BETAOXIDATION	5.92	2.72
AGEING_BRAIN_UP	5.68	3.71
ASTON_OLIGODENDROGLIA_MYELINATION_SUBSET	5.57	3.74
ICHIBA_GVHD	5.55	4.23
HUMAN_MITODB_6_2002	5.29	2.78
MITOCHONDRIA	5.23	3.57
WIELAND_HEPATITIS_B_INDUCED	5.18	0.03
VALINE_LEUCINE_AND_ISOLEUCINE_DEGRADATION	5.12	2.64
EMT_UP	5.00	3.15
JECHLINGER_EMT_UP	4.89	2.93
CORDERO_KRAS_KD_VS_CONTROL_UP	4.87	2.30

Pathway name	Z score	
	7 DIV vs. control	3 DIV vs. control
DAC_IFN_BLADDER_UP	4.78	0.94
STEMCELL_EMBRYONIC_UP	4.78	1.46
STEMCELL_HEMATOPOIETIC_UP	4.69	2.82
ASTON_DEPRESSION_DOWN	4.67	2.35

The 20 most strongly downregulated or upregulated pathways after 7 days of TTX treatment ranked according to their Z score. Z scores after 3 days of TTX treatment are listed for comparison. Pathways are from the MSIG database of the BROAD Institute of MIT (Subramanian et al., 2005).

Key: BROAD,; DIV, days in vitro; MIT,; MSIG,; TTX, tetrodotoxin.